ISBN: 978-984-34-8313-3
www.iabse-bd.org

Comparative seismic vulnerability assessment of shape memory alloy (SMA) and steel reinforced concrete (RC) bridge piers

M.A. Hawraneh & M.S. Alam
The University of British Columbia, Kelowna, BC, Canada

A.H.M.M. Billah
Lakehead University, Thunder Bay, ON, Canada

ABSTRACT: In recent years, the application of shape memory alloy (SMA) as reinforcement in concrete structures has attracted a lot of attention among researchers and practitioners. SMAs' unique characteristics such as super-elasticity, shape memory effect, and hysteretic damping, make them appropriate for bridge engineering applications in high seismic zones. Recent earthquake events have shown that the near-fault ground motions could be quite devastating to infrastructure. Besides, long-duration ground motions have attracted a lot of interest due to the duration effect on structural response, which could lead to substantial damages. This study aims to evaluate the comparative seismic fragility of concrete bridge piers reinforced with SMA rebars and steel rebars in the plastic hinge region under long duration and near-fault earthquakes. The bridge pier is assumed to be part of a lifeline bridge located in Western Canada and has been designed following a performance-based design approach. Seismic vulnerability of the SMA and Steel reinforced concrete (RC) bridge piers has been assessed through fragility analysis considering uncertainty in the material properties and the seismic hazard of the site location. Fragility curves are developed using suits of long duration and near-fault ground motions where each suite contains 20 ground motions. The vulnerability of the bridge piers has been evaluated in terms of maximum drift. The outcome of this study indicates how the performance of the SMA-RC bridge pier and steel-RC bridge pier are affected by the duration of ground motion and fault location.

1 INTRODUCTION

During the past years, the world encountered several high magnitude and long period earthquake events with catastrophic impact. Seismologists are expecting devastating earthquake with high magnitude to hit Canada's west coast (Insurance Bureau of Canada 2013) which could have severe impact on the highway network. Bridges are an important part of the highway network of any country, therefore maintaining them safe and functioning is very important. Bridges are considered as critical structures due to their high vulnerability to seismic events (Cruz & Saiidi 2012). Currently, researchers are exploring the application of innovative structural materials and systems in bridge piers to make them more resilient and improve their seismic performance to keep bridges operational even after a major seismic event. To achieve that, researchers have proposed several innovative solutions such Shape Memory Alloy (SMA) rebars (Youssef et al. 2008). The unique characteristics of super-elastic SMA to retrieve its pristine shape after undergoing extensive deformation will reduce the residual drift, making it a convenient replacement for steel reinforcement in RC structures.

Various researchers investigated the feasibility of utilizing SMAs in protecting structures against seismic events (Carreras 2011). Saiidi & Wang (2006)investigated the effectiveness of reinforcing bridge piers with SMA rebar in the plastic hinge region using shake table tests. Other studies found that using SMA in the plastic hinge region of concrete structures could decrease induced damage from a seismic event while dissipating energy adequately (Billah & Alam 2015).However, very limited information is currently available in the literature that compares the vulnerability of highway bridges subjected to long-duration (LD) ground motion and other types of ground motions such as near-fault events. Ou et al. (2014) found a lower ductility capacity for bridge piers subjected to LD. Recently, seismic events such Chile earthquake (2010), and Tohoku earthquake (2011) revealed the vulnerability of existing structures under LD earthquakes On the other hand,Near Fault (NF) ground motions have unique characteristics as they apply high input energy on

structures through pulse-like loading while incorporating high ground displacement, long period velocity pulse and peak velocities(Somerville 2002).Billah et al. (2013) found that NF ground motion could generate high ductility demand on the bridge. In another study, Al-Hawarneh et al. (2020)found that LD ground motions had a greater impact on strength and stiffness deterioration of the bridge pier due to longer applied loading. Iervolino et al. (2006) found that the impact of ground motion duration on the energy dissipation capacity of the structure is huge due to the gradual strength degradation.

The objective of this study is to capture the influence of ground motion duration and pulse-like motions on the vulnerability of SMA-RC and steel-RC bridge piers using fragility curves. To address this issue, this study investigates the seismic fragility of SMA-RC and steel-RC bridge piers under 20 NF and 20 LD ground motions considering maximum drift as damage measures for the fragility curves. Moreover, this study considered the strength degradation of the bridge pier in the numerical modeling to obtain an accurate response of the structure under long duration motions. The results show that the ground motion characteristics significantly influence the bridge pier vulnerability.

2 BRIDGE PIER CHARACTERISTICS

Two reinforced concrete bridge piers with similar characteristics are considered in this study. However, they differ by reinforcement in the plastic hinge where one of them is reinforced with SMA rebar while the other one has conventional steel rebar in the plastic hinge region. The Steel-RC bridge pier is designed based on the performance-based design guidelines proposed by the Canadian Highway Bridge Design Code((CHBDC) 2014).However, SMA-RC bridge pier is designed following the design guidelines proposed by Billah & Alam (2016)due to the lack of design guidelines for SMA. The bridge piers are part of a three-span concrete girder bridge located in Vancouver, BC in site soil class-C (stiff soil). The superstructure is supported on a single column bent on a pile foundation. For simplicity in achieving the objectives of this study, the bridge piers are assumed to be fixed at the bottom. To simulate the boundary condition of the actual pier under seismic excitation, the column rotation is fixed at the top, but the movement is free (Billah & Alam 2016).The superstructures' mass contribution on the pier is represented 10% of the nominal pier axial capacity which is mass of 85 tons located at the pier top. The bridge under study is a lifeline bridge based on (CHBDC 2014) bridge classification. This study used various performance-based damage states as shown in Table 1.

Table 1. Damage states of bridge pier.

Damage State	Performance Level	Functional Level	Drift, Δ (%)	
			Steel-RC	SMA-RC
Slight (DS= 1)	Cracking	Fully Operational	0.88	0.28
Moderate (DS= 2)	Yielding	Operational	1.71	1.64
Extensive (DS= 3)	Initiation of Local Mechanism	Life safety	2.79	2.28
Collapse (DS= 4)	Strength Degradation	Collapse	3.24	7.65

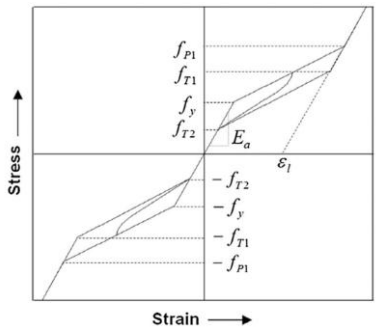

Figure 1.Super-elastic model of SMA (Auricchio& Sacco 1997)

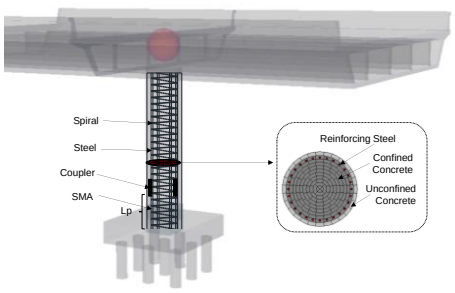

Figure 2. Pier geometry and cross-section

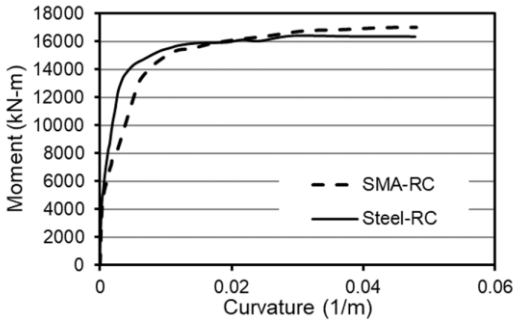

Figure 3. Moment curvature relationship ofsteel-RC and SMA-RC section.

The height and diameter of both bridge piers are 5m and 1 m, respectively. The bridge piers are designed using f_c'= 40 MPa for concrete, f_y= 435MPa for steel and f_y= 750 MPa. For SMA-RC bridge pier, Ferrous (FeNCATB) SMA rebar with an ultimate strain of 13.5% is utilized as longitudinal reinforcement in the plastic hinge of the SMA-RC pier. This type of SMA is used due to its comparable ultimate strain to the steel rebars ultimate strain. The parameters used to define the super-elastic SMA model are f_y (austenite to martensite starting stress), f_{P1}(austenite to martensite finishing stress), f_{T1} (martensite to austenite starting

stress), f_{T2} (martensite to austenite finishing stress), ε_s (maximum super-elastic strain) and, and E (modulus of elasticity) which are shown in Figure1. Table 2 shows the properties of the reinforcing material and concrete utilized in this study. Both piers are reinforced with 28-25M longitudinal rebars to meet the performance requirements. The transverse reinforcement consisted of 15M spiral at 75 mm pitch to satisfy the CHBDC seismic design and detailing requirements. Figure2 shows bridge pier's cross-section and geometry. The bridge piers are designed to have comparable moment capacities as shown in Figure 3.

Table 2. Material properties of the bridge.

Material	Properties		Material	Properties		Material	Properties	
Concrete	f_c' (MPa)	40.0	Steel	E_s (GPa)	200	SMA (FeNCATB)	E (GPa)	46.9
							ε_s%	13.5
	ε_c	0.0029		f_y (MPa)	435		f_y (MPa)	750
	f_t (MPa)	3.5		f_u(MPa)	692		f_{p1}(MPa)	1200
	E_c (GPa)	23.1		ε_s%	12		f_{T1} (MPa)	300
							f_{T2} (MPa)	200

3 FINITE ELEMENT MODELING

The piers are modeled using, SeismoStruct (2018), the fiber-based nonlinear finite element program. The bridge piers are molded using 3-D inelastic force-based beam-column elements.Fiber-based modeling with a distributed plasticity approach could accurately mimic the cyclic strength and stiffness degradation of structures when subjected to a long duration ground motion (Billah & Alam 2018).This study utilized the non-linear variable confinement model of Madas & Elnashai (1992) for concrete and the Menegotto-Pinto steel model (Menegotto 1973)with the Filippou & Bertero (1983) isotropic strain hardening property to model the reinforcing steel material. This steel mode considers low-cycle fatigue for steel bars (Fragiadakis & Papadrakakis 2008). Auricchio& Sacco (1997)constitutive relationship is used for SMA.

4 FRAGILITY FUNCTION METHODOLOGY

Fragility function expresses the conditional probability of a member/structure exceeding a certain damage threshold under a selected ground motion intensity (Porter et al. 2007).According to Alam et al. (2012),many researchers preferred to generate fragility curves using the analytical method since it requires less or no actual damage data. Various analytical methods have been proposed and used to generate fragility curves such as probabilistic seismic demand models and nonlinear static analysis (Bhuiyan & Alam 2012). In order to develop analytical fragility curves, it is required to develop structural capacity and demand models. The fragility function is described as following (Billah & Alam 2015).

$$Fragility = P[LS|IM=y] \quad (1)$$

where *IM* is the ground motion intensity measure, *y* is the ground motion intensity measure realized condition and *LS* is the damage state of the structure.

In this study, the functional relationship between the *IM* and engineering demand parameter *(EDP)* is determined using a probabilistic seismic demand model *(PSDM)*. The nonlinear time-history analyses of the bridge piers are used for generating the (*PSDM*). Moreover, the peak ground acceleration (*PGA*) is considered as the intensity measure (*IM*), whereas maximum drift (%) of the bridge pier is used as the *EDP*s.

This study adopts the cloud approach in developing bridge piers' seismic fragility curves. For the cloud approach, the standard deviation and mean corresponding to each limit state is obtained through a regression analysis that assumes a power-law function (Cornell et al. 2002).This generates a logarithmic correlation between the *EDP* and median *IM*.

$$EDP = a\,(IM)^b \text{ or, } \ln(EDP) = \ln(a) + b\ln(IM) \quad (2)$$

Where *a* and *b* are estimated from a regression analysis of the time history analyses results. In this study, *IDA* is carried out to generate adequate damage data for the cloud approach to develop *PSDM* (Billah et al. 2013).The *IDA* is performed to generate 400 data sets by scaling every single ground motion of each suit to 20 increments to be used in the regression analysis. The dispersion of the demand, $\beta_{EDP|IM}$ under a specific *IM* is estimated using Eq. 2 (Baker & Cornell 2006).

$$\beta_{EDP|IM} = \sqrt{\frac{\sum_{i=1}^{N}\left(\ln(EDP) - \ln\left(aIM^{b}\right)\right)^{2}}{N-2}} \quad (3)$$

Where, N= total number of simulations. Through utilizing the *PSDM* and limit state for each damage level, the fragility curves are developed using the following equation (Padgett & DesRoches2008).

$$P[DS \mid IM] = \phi\left[\frac{\ln(IM) - \ln(IM_n)}{\beta_{comp}}\right] \quad (4)$$

Where, Φ[ ] is the standard normal cumulative distribution function (*CDF*) and

$$\ln(IM_n) = \frac{\ln(S_c) - \ln(a)}{b} \quad (5)$$

IM_n represents the median value of *IM* for a particular damage state (slight, moderate, extensive, and collapse). Whereas a and b are *PSDMs'* regression coefficients. Eq.5 expresses the dispersion component (Padgett &DesRoches2008).

$$\beta_{comp} = \frac{\sqrt{\beta_{EDP|IM}^2 + \beta_c^2}}{b} \quad (6)$$

Where, β_c and S_c represent the dispersion and the median value for a particular damage state of bridge pier, respectively. The bridge piers limit state capacities in terms of lognormal standard deviation (βc) and median (*Sc*) are presented in Table 3.The coefficient of variation (*COV*) accounts for the associated uncertainty of each damage state. For lower damage states (*slight* and *moderate*), a value of 0.25 is assumed for the COV_{slight} and $COV_{moderate}$; however, for higher damage state (*extensive* and *collapse*), a higher value for the *COV* is assigned ($COV_{extensive} = COV_{collapse} = 0.5$) (Porter et al. 2007).

Table 3. Limit state capacity of SMA-RC and steel-RC bridge pier.

Damage	Steel-RC		SMA-RC	
state	*Sc*	*βc*	*Sc*	*βc*
Slight	0.89	0.25	0.28	0.25
Moderate	1.71	0.25	1.64	0.25
Extensive	2.79	0.50	2.28	0.50
Collapse	3.24	0.50	7.65	0.50

5 FRAGILITY ASSESSMENT OF SMA-RC AND STEEL-RC BRIDGE PIER

This study utilized the fragility assessment to capture the influence of ground motion duration along with various reinforcement configurations on the seismic performance of the bridge piers. The following section describes the procedure followed to perform the fragility assessment for both bridge piers.

5.1 *Ground Motion Selection*

This study used 40 ground motion records obtained from the Pacific Earthquake Engineering Research (PEER) center database (Baker et al. 2011).The records represent 20 NF and 20 LD medium to strong ground motions with various magnitudes and PGA. The PGA values for the NF ground motions ranged from 0.37 g to 1.07 g and 0.1 g to 2.07 g for the LD ground motions. This study utilized the ground motions with an epicentral distance less than 10 km as NF motions. On the other hand, LD ground motion is identified by their significant duration. One of the most used methods to differentiate LD duration from other types of ground motion is Arias significant duration (Bommer & Martinez-Pereira 1990).This study used the same set of LD and NF ground motion records used by Al-Hawarneh et al. (2020).

5.2 *Development of Fragility Curve*

This study uses *IDA* to obtain the probability of exceeding a certain damage state for NF and LD ground motions. The peak response (maximum drift) for each analysis is plotted alongside the corresponding *IM* for

each ground motion. Padgett & Des Roches(2008) and Mackie & Stojadinovi¢ (2007) suggested that the PGA is the best *IM* to describe the earthquake ground motion severity. The efficiency of *IM*s could be assessed by dispersion $\beta_{EDP|IM}$ (Padgett &DesRoches2008). However, the practicality is measured by the regression parameter *b* in the *PSDM* Eq. 2. A higher value of *b* indicates a more practical *IM*(Padgett &DesRoches2008).

5.3 *PSDMs for Maximum Drift*

The *PSDM*s are developed utilizing regression analysis of the bridge piers' maximum drift demand obtained from *IDA.PSDM*s for both bridge piers subjected to NF and LD ground motions in terms of the maximum drift (%) as the EDP are shown in Figure4. The *PSDM*s are generated using a large number of demand values for the given *IM*. Finally, the parameters $\beta_{EDP|IM}$, *a*, and *b* are estimated using linear regression analysis. Table 6 shows a comparison of the influence of different ground motions and reinforcement configurations on the demand models. The results for the NF ground motions show that the SMA-RC bridge pier experienced a slight increase in the demand dispersion ($\beta_{D|IM}$) by 9% compared to the steel- RC bridge pier. Moreover, the regression models show an 8% lower slope *(b)* for the SMA-RC bridge pier compared to the steel-RC bridge pier, whereas the intercept (*ln(a)*) value is 10% higher for the SMA-RC bridge pier compared to the Steel-RC counterpart. This high intercept value indicates the lower median value of the demands on the SMA-RC pier as compared to the steel-RC bridge pier. However, the results for the LD ground motions show that the SMA-RC bridge pier exhibited a 55% increase in the demand ($\beta_{D|IM}$) as compared to the steel-RC bridge pier. The regression models show higher slope *(b)* value for the SMA-RC bridge pier by 19% and 14% lower intercept (*ln(a)*) values compared the Steel-RC bridge pier, indicating that the SMA-RC bridge pier tends to have a higher median value of the demands placed on the piers compared to the steel-RC.

Table 4. PSDMs for different ground motions.

Ground motion type	EDP	SMA-RC			Steel-RC		
		a	*B*	$\beta_{EDP\|IM}$	*a*	*B*	$\beta_{EDP\|IM}$
LD ground motion	Maximum Drift, Δ (%)	2.53	0.82	0.62	2.94	0.69	0.40
NF ground motion	Maximum Drift, Δ (%)	7.82	0.93	0.56	7.03	1.00	0.51

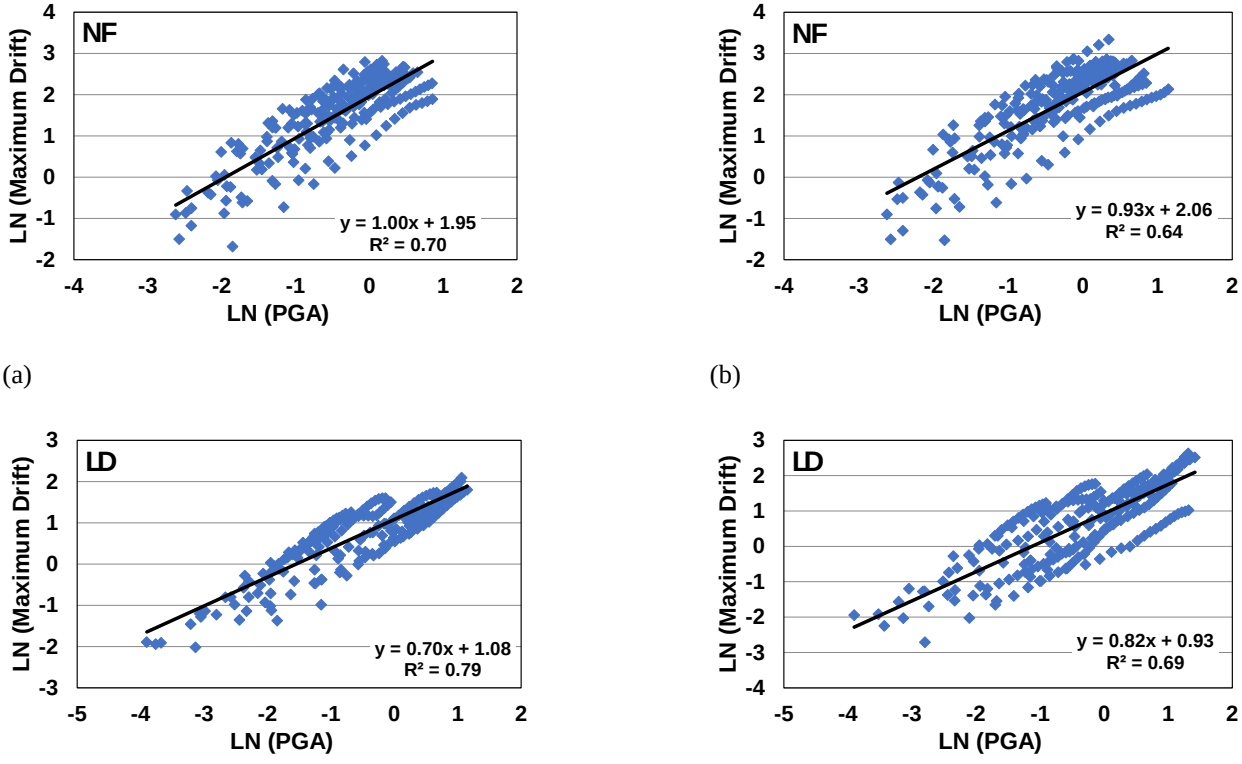

Figure 4. PSDMs for maximum drift for (a) steel-RC bridge pier for NF motions (b) SMA-RC bridge pier for NF motions, (c) steel-RC bridge pier for LD motions, (d) SMA-RC bridge pier for LD motions.

In contrast to LD motions, NF motions exhibit higher intercept (*ln(a)*) which is about 2.5and 3 times for the steel-RC bridge pier and the SMA-RC, respectively. Furthermore, the slope *(b)* value of the NF regression

model is higher by 13% and 44% for the SMA-RC bridge pier and the steel-RC bridge pier, respectively, compared to the LD regression model. This indicates an increase in the demand placed on the bridge components. The difference in the maximum drift (%) between SMA-RC and steel-RC bridge piers is primarily associated with the mechanical properties of steel and SMA (Table 2). SMA rebar's low elastic modulus resulted in a lower pier stiffness thus, higher displacement for the SMA-RC bridge pier and eventually a higher maximum drift (%) for the SMA-RC bridge pier compared to the Steel-RC bridge pier.

5.4 *Maximum Drift Fragility Curves*

The developed fragility curves offer valuable insight on the effect of ground motion type as well the influence of using SMA rebar on the probability of damage. The fragility is directly approximated from the *PSDM* parameters, regression analysis as well as the limit state capacity of each damage state. The fragility curves are developed utilizing the parameter identified in Eq.4.

The assessment of the fragilities as shown in Figure5indicates that for NF ground motion the SMA-RC bridge pier is more vulnerable than the Steel-RC bridge pier from DS=1 (*slight)* to DS =3 *(extensive)*. Conversely, the steel-RC bridge pier tends to have higher vulnerability for DS=4 (*collapse*) compared to the SMA-RC pier. This can be attributed to the significantly higher limit state of SMA-RC pier for DS=4 as compared to the steel counterpart (Table 1). Figure5illustrates that SMA is more effective at higher damage states as compared to the steel reinforcement when subjected to NF ground motions.

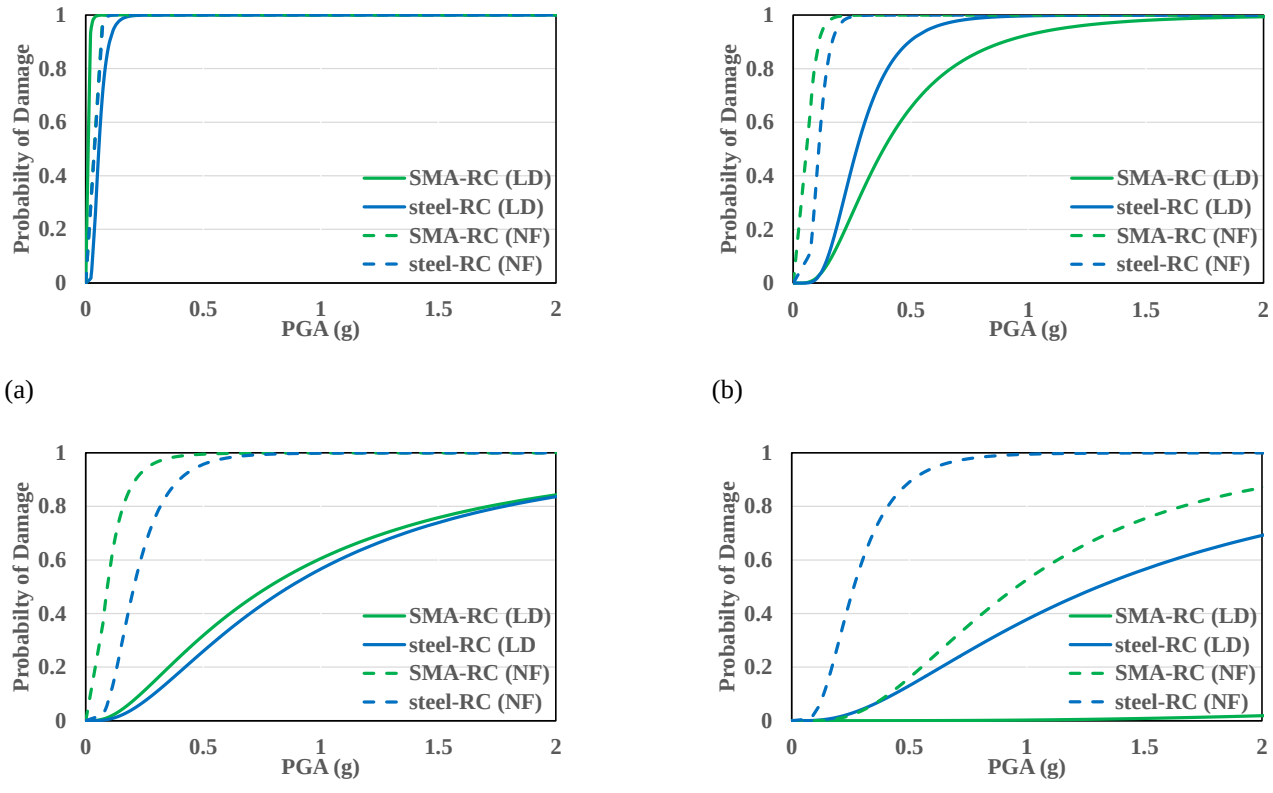

Figure 5. Comparison of fragility curves for SMA-RC and steel under LD and NF ground motion for various damage states considering Maximum drift as *EDP*, (a) slight damage state, (b) moderate damage state, (c) extensive damage state, (d) collapse damage.

In order the compare the collapse probability for both bridge piers, the design PGA (0.46g) of the bridge piers that corresponds to a 2% probability of exceedance in 50 years is considered as the reference PGA. The collapse probability under NF ground motion at PGA of 0.46gfor SMA-RC pier is 13% whereas it is86% for the Steel-RC pier. At the highest damage level (collapse), the SMA-RC bridge pier has significantly lower vulnerability compared to the steel-RC bridge pier. Figure5indicates that at low to medium intensities, the Steel-RC bridge pier has a lower probability of damage compared to SMA-RC pier. Since it has higher stiffness compared to the SMA-RC pier, it experiences less deformation. Although the SMA-RC bridge pier will undergo higher deformation compared to the Steel-RC pier, yet the collapse vulnerability of the Steel-RC pier is higher than the SMA-RC bridge pier due to the higher limit state capacity of the SMA-RC, almost

twice that for the Steel-RC bridge pier as shown in Table 1. The higher limit state values of the SMA-RC pier are associated with the mechanical properties of SMA as shown in Table 2, in particular, the ultimate stress and strain of SMA.

On the other hand, for LD ground motions, Figure. 5illustrates the fragility curves for both bridge piers considering maximum drift (%) as the *EDP*. The fragility curves illustrated in Figure5indicate that the SMA-RC bridge pier exhibited higher vulnerability under the LD motions for DS=1 and DS=3. From Figure5it can be observed that as the damage state goes higher, the difference between the vulnerabilities of the two bridge piers gets reduced. Subsequently, at DS=4 (*collapse)* the SMA-RC pier significantly outperformed the Steel-RC pier. For example, the collapse probability at design PGA (0.46 g) is 11% for the steel-RC piers whereas it is around 0.1% for the SMA-RC pier as shown in Figure 5.

The comparison of the fragility curves for LD and NF ground motions for the same bridge pier type indicates that the NF ground motion cause higher vulnerability for all damage states *(slight, moderate, extensive, and collapse)* compared to LD ground motions under the same intensity (Figure 5). Figure 5shows that the collapse probability for the SMA-RC bridge and the steel-RC piers under the NF ground motions at the design PGA (0.46 g) is 11% and 86%, respectively. Whereas, for the LD ground motions, the collapse probability at the design PGA (0.46 g) is 0.1% and 13% for the SMA-RC and the steel-RC bridge pier, respectively. This highlights the benefit of using SMA rebar in high seismic zones that can experience either long duration or near-fault motions.

6 CONCLUSIONS

Seismic vulnerability for SMA-RC and Steel-RC bridge piers assessed by fragility curves developed using analytical simulation under two different suits of ground motions. A probabilistic framework is adopted to evaluate the relative vulnerability of two bridge piers considering maximum drift as the *EDP*. The IDA-based cloud approach is implemented to produce the needed data for the fragility analysis. The following conclusions are driven from numerical results:

- The fragility assessment of the bridge piers considering maximum drift as *EDP* showed that NF ground motions resulted higher vulnerability compared to LD ground motions for both reinforcement types and all damage states.
- Implementing SMA in the plastic hinge region had a greater impact on the reduction of the LD ground motion collapse vulnerability compared to NF ground motion. The probability of collapse for SMA-RC pier under LD ground motion at PGA of 0.46g is 0.1% whereas it is 13% under NF ground motion.
- For NF ground motion, SMA-RC bridge piers had slightly higher vulnerability for all damage states except DS=4 (*collapse*) compared to the steel-RC bridge pier where it is significantly lower. The PGA of exceeding 50% collapse probability for the SMA-RC bridge pier is 0.96g compared to 0.26g for the steel-RC bridge piers.
- For LD ground motions, SMA-RC bridge pier's vulnerability is higher compared to the Steel-RC bridge pier at DS 1 and DS 3 however, it is lower for DS 2 and DS 4. The PGA of exceeding 50% collapse probability for the SMA-RC bridge pier is around 3 times higher than that for steel-RC bridge pier indicating a significantly higher collapse vulnerability for Steel-RC bridge pier.

REFERENCES

Alam, M. S., Bhuiyan, M. R., & Billah, A. H.M.M., (2012). Seismic fragility assessment of SMA-bar restrained multi-span continuous highway bridge isolated by different laminated rubber bearings in medium to strong seismic risk zones. *Bulletin of Earthquake Engineering, 10*(6), 1885-1909.

Al-Hawarneh, M., Billah, A.H.M.M., & Alam, M. S. (2020). Seismic Fragility Assessment of Shape Memory Alloy Reinforced Concrete Bridge Piers under Long Duration and Near-Fault Ground Motions. *Special Publication, 341*, 131-159.

Auricchio, F., & Sacco, E. "A superelastic shape-memory-alloy beam model." Journal of intelligent material systems and structures, 1997, pp.489-501.

Baker, J. W., &Cornell, C. A. (2006). *Vector-valued ground motion intensity measures for probabilistic seismic demand analysis*. Pacific Earthquake Engineering Research Center, College of Engineering, University of California, Berkeley.

Baker, J. W., Lin, T., Shahi, S. K., & Jayaram, N. (2011). New ground motion selection procedures and selected motions for the PEER transportation research program. *PEER report, 3*.

Bhuiyan, A.R., & Alam, M. S. (2012). Seismic vulnerability assessment of a multi-span continuous highway bridge fitted with shape memory alloy bars and laminated rubber bearings. *Earthquake Spectra, 28*(4), 1379-1404.

Billah, A.H.M.M., & Alam, M. S. (2018). Probabilistic seismic risk assessment of concrete bridge piers reinforced with different types of shape memory alloys. *Engineering Structures, 162*, 97-108.

Billah, A. H. M. M., & Alam, M. S. (2016). Performance based seismic design of concrete bridge pier reinforced with Shape Memory Alloy-Part 1: Development of Performance-Based Damage States. *ASCE J. Struct. Eng*, *142*(12), 1-11.

Billah, A. H. M.M., & Shahria Alam, M. (2015). Seismic fragility assessment of highway bridges: a state-of-the-art review. *Structure and Infrastructure Engineering*, *11*(6), 804-832.

Billah, A. H. M.M., & Alam, M. S. (2015). Seismic fragility assessment of concrete bridge pier reinforced with superelastic shape memory alloy. *Earthquake Spectra*, *31*(3), 1515-1541.

Billah, A. H. M.M., Alam, M. S., &Bhuiyan, M. R. (2013). Fragility analysis of retrofitted multicolumn bridge bent subjected to near-fault and far-field ground motion. *Journal of Bridge Engineering*, *18*(10), 992-1004.

Bommer, J. J., &Martinez-Pereira, A. (1999).The effective duration of earthquake strong motion. *Journal of earthquake engineering*, *3*(02), 127-172FFF.

Canadian Standards Association. (2014). Canadian highway bridge design code (CAN/CSA S6-14). *Toronto, Ontario*.

Carreras, G., Casciati, F., Casciati, S., Isalgue, A., Marzi, A., & Torra, V. (2011). Fatigue laboratory tests toward the design of SMA portico-braces. *Smart Structures and Systems*, *7*(1), 41-57.

Cornell, C. A., Jalayer, F., Hamburger, R. O., & Foutch, D. A. (2002). Probabilistic basis for 2000 SAC federal emergency management agency steel moment frame guidelines. *Journal of structural engineering*, *128*(4), 526-533.

Cruz Noguez, C. A., & Saiidi, M. S. (2012). Shake-table studies of a four-span bridge model with advanced materials. *Journal of Structural Engineering*, *138*(2), 183-192.

Filippou, F. C., Popov, E. P., & Bertero, V. V. (1983).Modeling of R/C joints under cyclic excitations. *Journal of Structural Engineering*, *109*(11), 2666-2684.

Fragiadakis, M., & Papadrakakis, M. (2008). Modeling, analysis and reliability of seismically excited structures: computational issues. *International journal of computational methods*, *5*(04), 483-511.

Hachem, M. M., Moehle, J. P., & Mahin, S. A. (2003). *Performance of circular reinforced concrete bridge columns under bidirectional earthquake loading*. Berkeley, CA: Pacific Earthquake Engineering Research Center.

Iervolino, I., Manfredi, G., & Cosenza, E. (2006). Ground motion duration effects on nonlinear seismic response. *Earthquake engineering & structural dynamics*, *35*(1), 21-38.

Mackie, K. R., & Stojadinović, B. (2007). Performance-based seismic bridge design for damage and loss limit states. *Earthquake engineering & structural dynamics*, *36*(13), 1953-1971.

Madas, P., &Elnashai, A. S. (1992).A new passive confinement model for transient analysis of reinforced concrete structures. *Earthquake Engineering and Structural Dynamics*, *21*(5), 409-431.

Menegotto, M. (1973). Method of analysis for cyclically loaded RC plane frames including changes in geometry and non-elastic behavior of elements under combined normal force and bending. In *Proc. of IABSE symposium on resistance and ultimate deformability of structures acted on by well defined repeated loads* (pp. 15-22).

Ou, Y. C., Song, J., Wang, P. H., Adidharma, L., Chang, K. C., & Lee, G. C. (2014). Ground motion duration effects on hysteretic behavior of reinforced concrete bridge columns. *Journal of Structural Engineering*, *140*(3), 04013065.

Padgett, J. E., & DesRoches, R. (2008). Methodology for the development of analytical fragility curves for retrofitted bridges. *Earthquake Engineering & Structural Dynamics*, *37*(8), 1157-1174.

Porter, K., Kennedy, R., & Bachman, R. (2007). Creating fragility functions for performance-based earthquake engineering. *Earthquake Spectra*, *23*(2), 471-489.

Saiidi, M. S., & Wang, H. (2006). Exploratory study of seismic response of concrete columns with shape memory alloys reinforcement. *ACI Materials Journal*, *103*(3), 436.

SeismoSoft, (2018).SeismoStruct - A computer program for static and dynamic nonlinear

Worldwide, A. I. R. (2013).Study of impact and the insurance and economic cost of a major earthquake in British Columbia and Ontario/Québec. *Insurance Bureau of Canada*, *345*

Youssef, M. A., Alam, M. S., & Nehdi, M. (2008). Experimental investigation on the seismic behavior of beam-column joints reinforced with superelastic shape memory alloys. *Journal of Earthquake Engineering*, *12*(7), 1205-1222.